International Journal of Engineering Research-Online
A Peer Reviewed International Journal
Articles available online http://www.ijoer.in

Vol.1., Issue.4, 2013

RESEARCH ARTICLE

ISSN:2321-7758

SYNTHESIS AND CHARACTERIZATION OF Ni-Al FERRITE NANOPARTICLES BY SOL-GEL TECHNIQUE AND ITS POTENTIALITY IN FLUORIDE ION REMOVAL FROM AQUEOUS SOLUTION

THUMMAPUDI NIRANJAN KUMAR[1], CH. VIJAY ANIL DAI[2] K.SURESH[3]

[1]Lecture in physics, AMAL College Anakapalli, Visakhapatnam, Andhra Pradesh
[2]Lecture in physics, A.G & S.G Siddhartha College of Arts and Science, Vuyyuru, Krishna, A.P
[3]Lecture in Physics, VSR & NVR Degree College, Tenali, Guntur Dist., A.P., India

Article Received: 08/09/2013 | Article Revised: 14/10/2013 | Article Accepted: 02/12/2013

ABSTRACT

Ni–Al ferrite with composition of Ni $Al_xFe_{2-x}O_4$ (x=0.0, 0.5, & 1.5) were prepared by citrate gel method. The prepared nanoferrites tested for the removal of Fluoride ion in aqueous media. Nanoferrite samples were characterized by X-ray powder diffraction (XRD), Fourier transform infrared spectroscopy (FTIR), and scanning electron microscopy (SEM). XRD analysis confirms the formation of pure single phases of cubic ferrites with average crystallite size of 18.64 nm. Kinetics and isotherm adsorption studies for adsorption of Fluoride ion were carried out. The experimental data of the isotherms were well fitted to the Langmuir isotherm model. It is expected that this kind of Ni-Al-Fe_2O_4 spinel ferrite nanoparticles has a potential application in water treatment fields due to its sensitive magnetic response properties and high catalytic activity.

Introduction

Spinel ferrites play an important role in technological applications. Their interesting electrical, magnetic, and dielectric properties make them useful in many applications, such as electronic devices, sensors, memory devices, data storage, and telecommunications[1]. Recently, the possibility of preparing ferrites in the form of nanoparticles (NPs) has opened a new and exciting research field with revolutionary applications, not only in electronic technology but also in the fields of biotechnology and water treatment[2], due to their nanometer size, superparamagnetic properties, and a high surface-to-volume ratio[3]. In recent years, NPs have been applied for removing heavy metals and organic/inorganic pollutants from aqueous solutions[4].

It is well known that the properties of ferrite materials strongly depend on the synthesis method. Different procedures for ferrite synthesis are described in the literature, including coprecipitation, low-temperature combustion synthesis, sol-gel, mechanical alloying, mechanical activation, and solid-state synthesis[5]. The mechanochemical synthesis can deliver the desired phases and structures in a single step, with high-energy milling conducted in an enclosed activation chamber at room temperature[6]. Usually, the complete formation of spinel ferrites was obtained only after milling followed by sintering, that is, by employing two

processing steps. It has been shown that the combined mechanochemical-thermal treatment yields a well ordered spinel phase in ferrites at lower annealing temperatures and shorter durations than those required in conventional ceramic methods[7].

Very low doses of fluoride (<0.5 mg/l) in water can induce tooth decay. However, higher doses (>1.5 mg/l), can lead to dental fluorosis or mottled enamel and excessively high concentration (>3.0 mg/l) of fluoride may cause skeletal fluorosis[8]. Fluoride poisoning can be prevented or minimized by using alternative water sources. Defluoridation of groundwater is one of the feasible options to overcome the problem of excessive fluoride in drinking water. Among the available techniques adsorption is still one of the most extensively used and cheapest methods for defluoridation of water. Literature research has shown that alumina supported on carbon nanotubes (Al_2O_3/CNT) has a saturation adsorption capacity of 39.4 mg/g fluoride uptake. It is also found that the adsorption capacity of Al_2O_3/CNT is 3.0 - 4.5 times that of γ-Al_2O_3 while almost equal to that of IRA-410 polymeric resin at 25˚C[9].

The purpose of this work is to synthesis the Ni-Al nanoferrites and to understand the influence of Al^{3+} ion substitution for a fixed Ni^{2+} ion concentration on the structural properties of Nickel nanoferrites. In this article, we investigated the effectiveness of one of prepared derivative of nickel aluminium nanoferrite ($NiAl_{0.5}Fe_{1.5}O_4$) obtained by sol-gel method, for removing fluoride ion from aqueous media.

Materials and methods

Chemicals

All reagents and chemicals used in the present investigation were of AR grade purchased from Ranbaxy/SD fine/ sigma Aldrich and all solutions were prepared by using fluoride free double distilled water

Synthesis of Ni $Al_xFe_{2-x}O_4$ (x = 0.0, 0.5,1.5)

Analytical grade (AR) with 98% purity of chemical reagents such as AluminumNitrate-98%Pure (AR Grade) $Al(NO_3)_3.9H_2O$, FerricNitrate-98%pure(ARgrade) $Fe(NO_3)_2$ $9H_2O$, Nickel nitrate –98% pure (AR grade) Ni $(NO_3)_2$ $6H_2O$ (AR), Citric acid - 98% pure (AR grade) ($C_6H_8O_7.H_2O$) & Ammonia - 98% pure (AR grade) NH_3 were used for the preparation of aluminium substituted Ni^{2+} nanoferrites of general formula Ni $Al_xFe_{2-x}O_4$ (x = 0.0, 0.5, 1.5) using sol-gel method. Stoichiometric chemical reagents were dissolved in de-ionized water. Mixed nitrate solution was magnetically stirred for an hour then citric acid was added to nitrate solution in 3:1 molar ratio and further stirred for 2 hours at 70°C temperature. Liquid ammonia was added to citric solution to maintain PH value at 7.0 and by continuously stirring on the hot plate at 100°C to get a viscous gel. The gel was kept on heating till it burns and undergoes combustion. As a result of auto-combustion finally fluffy powder of synthesized ferrite was obtained. The fine powder was calcined under the constant heating conditions at 700°c for 6 hours and grinded into fine particles. Finally, the calcined fine powder was pressed into pellets of 10 mm diameter and approximately 1-2 mm thickness.

Structural characterization

X-Ray Diffraction (XRD): X-ray diffraction is now a common technique for the study of crystal structures and atomic spacing. The patterns for the Ni-Al nanoferrites were recorded using an X-ray diffractometer (PANLYTICAL) using secondary monochromatic Cu K radiation of wavelength l = 0.1541 nm at 40 Kv/50 mA in the scan range 2q = 20˚ to 90˚. Samples were supported on a glass slide.

Scanning Electron Microscopy (SEM): Morphology of the samples was investigated using scanning electron microscope (model JSM-7000F) which also has been used for compositional analysis of the prepared Ni-Al nanoferrites nanoparticles. A drop of nanoparticles dissolved in methanol was placed on a copper grid.

Fourier Transform Infrared Spectroscopy (FTIR): The fourier transform infrared (FTIR) absorption spectra of the samples were recorded using FTIR spectrometer (Thermo Nicolet, Avatar 370) in the wave number range 4000–400 cm^{-1} with Potassium bromide (KBr) as binder.

Defluoridation: 100 ml of standard fluoride solution (5 mg/L) was pipette out into a 500 ml beaker. To it, 0.5g/L of the prepared Ni-Al nanoferrite (Ni $Al_{0.5}$ $Fe_{1.5}O_4$) was added and stirred at 200 rpm mechanically for 30 minutes. Then, the solution was filtered through Whatman No- 42 filter paper. The F-ion concentration in the

sample after defluoridation was determined using ion-selective electrode (Orion ion selective electrode) specific to fluorides. The same procedure was adopted for the experiments carried out by varying other parameters. Batch Mode Adsorption experiments were carried out to investigate the adsorption efficiency at varied initial concentration (1-10 mg/L), pH (2.0-12.0) and contact time (10-90min.). All the experiments were performed at room temperature of 30±1°C[10]. The amount of Fluoride taken up and the percentage of removal of the F-ion by the adsorbent were calculated by applying Eqn. 1 and 2, respectively:

$$q=\frac{(C_o-C_f)}{m}.V \qquad \text{.....(Eqn 1)}$$

$$\%Removal=100.\frac{(C_o-C_f)}{C_o} \qquad \text{.....(Eqn 2)}$$

where q is the amount of dye taken up by the adsorbent (mg g^{-1}), C_o is the initial F^- concentration put in contact with the adsorbent (mg L^{-1}), C_f is the dye concentration (mg L^{-1}) after the batch adsorption procedure, m is adsorbent mass (g) and V is the volume of the F^- solution (L).

Results and discussion

Structural characterization

XRD analysis: The XRD patterns of synthesized nickel ferrite nanoparticles are depicted in figure 1. It confirms the formation of single phase spinel structure for all the samples. The formation of spinel cubic structure can be confirmed by the existence of (311), (400), (422), (511) and (440) crystal planes in the XRD patterns, which is in accordance with the JCPDS powder diffraction file. The strongest reflection comes from (311) which denotes the spinel plane[11]. The particle size was determined for all the samples based on high intensity (311) plane using Scherer formula. The average particle size was found to be 18.05 nm.

Table 1: Crystalline properties of Ni $Al_xFe_{2-x}O_4$ (x = 0.0, 0.5,1.5)

Composition (x)	Lattice constant (a) (Å)	X-ray density(ρx) (gm/cm^3)	Bulk density (ρB) (gm/cm^3)	Porosity (ρ) (%)	Crystallite size (t) (Debye-Scherer) (nm)
0	8.751	5.112	3.973	23.39	18.75
0.5	8.743	5.093	4.088	21.23	18.05
1.5	8.730	5.084	4.100	20.32	16.88

The average crystallite size of the ferrite nanoparticles was calculated using the Debye-Scherrer equation[12]:

$$t=\frac{0.9\lambda}{\beta\cos\theta}$$

Where, λ is wavelength of the X-ray radiation, is full width at half maximum, β is Bragg's angle. It was found that the average crystallite size of the ferrite nanoparticles is in the range 18 to 16nm. It was noticed that the crystallite size and lattice constant gradually decreased with increasing Al^{3+} ion concentration (Table 1).

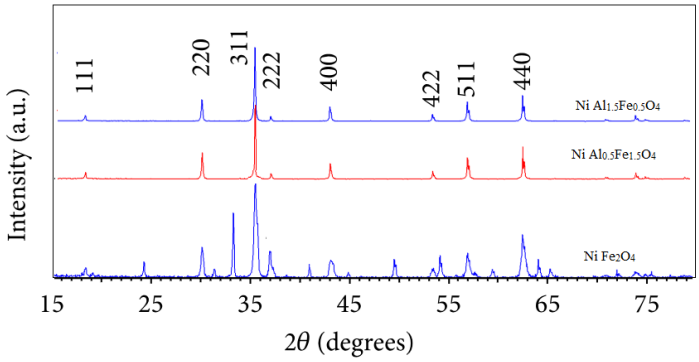

Figure 1: XRD patterns of Ni $Al_xFe_{2-x}O_4$ (x=0.0, 0.5, & 1.5) nanoferrites

The average crystallites size (d), the lattice parameter (a) etc parameters of the studied nickel-Al ferrites are also determined from the experimental XRD profiles (Table 1) by using the Williamson-Hall analysis. A well defined effect of the crystals size decrease and increase in the crystal defects and lattice parameter is observed for the mechanochemically obtained materials (Table 1). A dependence of the lattice parameter on the preparation method and the phase composition exists.

FT IR analysis: The FTIR spectra of prepared ferrites are shown in figure 2. Two peaks at the range 539-534cm^{-1} corresponds to intrinsic stretching vibrations of the metal at tetrahedral site and at 361-358 cm^{-1} corresponds to octahedral stretching confirms the formation of spinel ferrite structure[13].

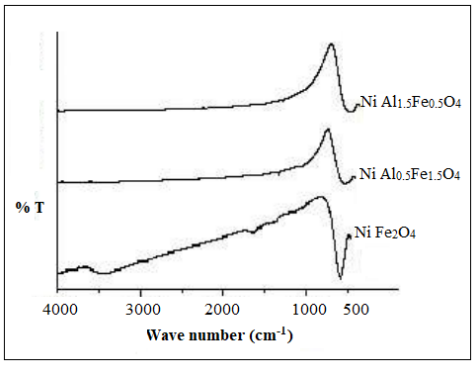

Figure 2: FT IR spectra of Ni $Al_xFe_{2-x}O_4$ (x=0.0, 0.5, & 1.5) nanoferrites

The presence of Al^{3+} ions in the tetrahedral site with a higher radius and atomic weight greatly influence the lattice distortions and make the Fe^{3+} ions to migrate and thus decreasing the octahedral and tetrahedral vibration frequency to a greater extent. This is clear from the spectra that as Aluminum content increases, these lattice vibrations are almost absent.

SEM analysis: Surface morphology and average grain size of Al^{3+} substituted nanoferrites were determined by using analytical scanning electron microscope by selecting 10,000 magnification range. SEM images (Figure 3) of typical samples Ni $Al_xFe_{2-x}O_4$ (x=0.0, 0.5, & 1.5) nanoferrites shows the nanocrystalline nature of ferrites with vivid pores suggesting it as more advantages for the adsorption applications. Intergranular diffusion can be clearly seen in SEM images of the ferrites. Fused grain nature can be seen in Ni $Al_xFe_{2-x}O_4$ (x=0.0, 0.5, & 1.5) nanoferrites (figure 3), whereas looks comparatively more crystalline affecting the spin coupling in ferrites which is at the base of the magnetic behaviour.

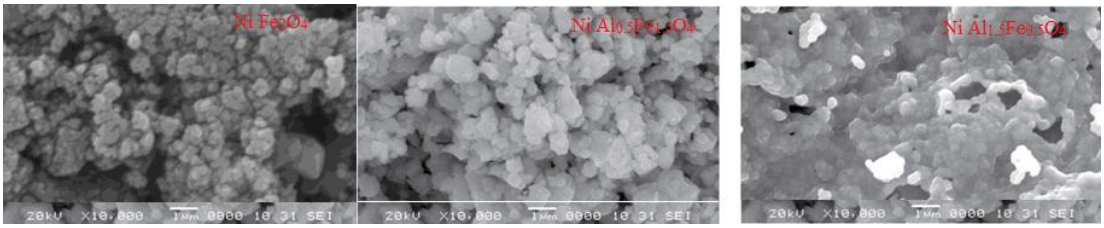

Figure 3: Scanning electron micrographs of Ni $Al_xFe_{2-x}O_4$ (x=0.0, 0.5, & 1.5) nanoferrites

Adsorption Studies

Effect of pH: The results of pH evaluation on fluoride removal by Ni-Al ferrites (NAF) was examined at different pH levels in the range of 2 to 12 is shown in Figure 4 and it was shown that the highest adsorption capacities were reached for the solutions with the lowest pHs. Figure 4 indicates the variation of adsorption at different pH levels. An examination of the figure indicates that maximum fluoride removal had occurred in strongly acidic medium and fluoride adsorption decreases with increase in pH. However, at neutral pH fluoride removal is considerably high, of the order of 78%. In the alkaline range, the fluoride adsorption remains slow. Higher adsorption rate of fluoride in the acidic range can be explained by the surface charge of the adsorbent.

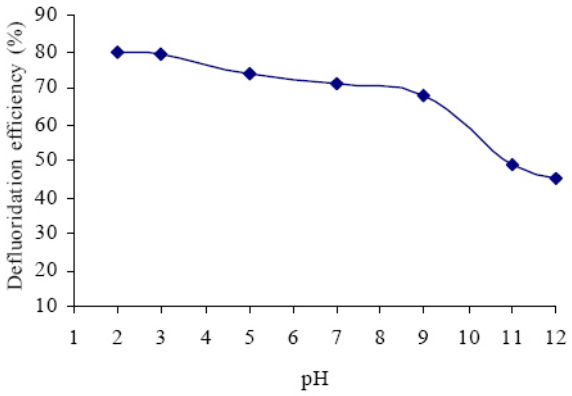

Figure 4 : Effect of pH on adsorption of Fluoride by NAF

Effect of Initial concentration of adsorbate (F^-) on concentration : The effect of increasing fluoride concentration on adsorption capacity of NAF is shown in Figure 5. For NAF adsorbent, the adsorption capacity increased to a specified level then attained equilibrium. The maximum adsorption capacity of NAF was 0.76 mg/g, when the initial fluoride concentration (Ci) was 5 mg/L.

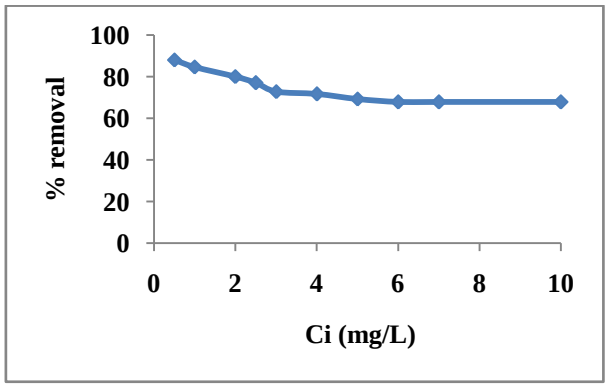

Figure 5: Effect of Fluoride ion concentration on adsorption by NAF

Isotherm study

The Freundlich equation

The empirically derived linearized Freundlich isotherm is defined as follows:

$\log q_e = \log K_f + 1/n \log C_e$

where K_f (L/g) and n (dimensionless) are the constants that can be related to the adsorption capacity and the adsorption nonlinearity intensity, respectively.

The values of K_f and $1/n$ may be calculated by plotting $\log q_e$ against $\log C_e$. The slope is equal to $1/n$ and the intercept is equal to $\log K_f$. Fig. 6, presents the plot of $\log q_e$ as a function of $\log C_e$ for the Fluoride removal.

Langmuir isotherm

The linearized Langmuir isotherm is written as follows:

$C_e / q_e = 1 / K_L q_m + C_e / q_m$

where q_m is the maximum monolayer adsorption capacity of the adsorbent (mg/g), and K_L is the Langmuir adsorption constant (L/mg), which is related to the free energy of adsorption.

The plot of C_e/q_e versus C_e gives a straight line with slope $1/q_m$, and intercept $1/K_L q_m$. Fig. 6, presents the plot of C_e/q_e vs C_e for the F^- removal by adsorption onto NAF

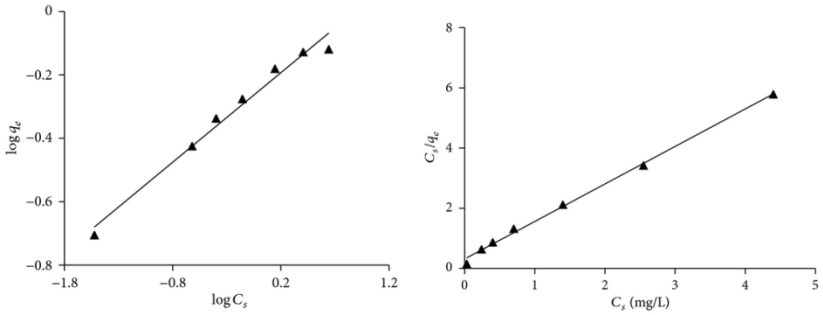

Figure 6: The Freundlich (left) and Langmuir isotherm (right) for fluoride adsorption using NAF

Table 2: Values of Freundlich and Langmuir isotherms constants.

	Freundlich constants			Langmuir constants		
Adsorbent	K_f	*n*	R^2	K	V_m	R^2
NAF	0.6	3.57	0.95	4	0.8	0.99

The Langmuir adsorption isotherm fitted very well for the fluoride adsorption on both adsorbents with the regression coefficient R^2 of 0.99 as shown in Figures 6. The values of the adsorption coefficient K and the monolayer capacity Vm calculated from the Langmuir equation are given in Table 2. The values of K and Vm are higher for NAF indicates that adsorption of fluoride on NAF is favorable. The Langmuir constant K can be used to predict whether an adsorption system is favorable or unfavorable[14]. For this purpose, a dimensionless separation factor R_L is generally employed.

$$R_L = \frac{1}{1 + aC_m}$$

where C_m is the initial concentration (10 mg/L, in this case) of Fluoride ion. The value of R_L indicates the type of the isotherm to be either unfavorable when $R_L > 1$, linear if $R_L = 1$, and favorable if $R_L < 1$ or $R_L = 0$. The calculated was 0.61 indicating that the adsorption of the F^- ion was a favorable process.

Effect of agitation time: The fluoride adsorption behaviour of the activated carbon of NAF is illustrated in figure 7. The effect of contact time on fluoride adsorption is shown in Figure 7. As the contact time increased, the adsorption capacity of both adsorbents also increased. The increase in the adsorption capacity in the first 30 minutes was very rapid. This might be due to the diffusion of fluoride ions into the surface pores of the adsorbents. After 40 minutes, the increase was less rapid probably due to the migration of fluoride ions from upper adsorbent surface to inner pores. NAF removed most of the fluoride ions around 40 minutes and then attained equilibrium.

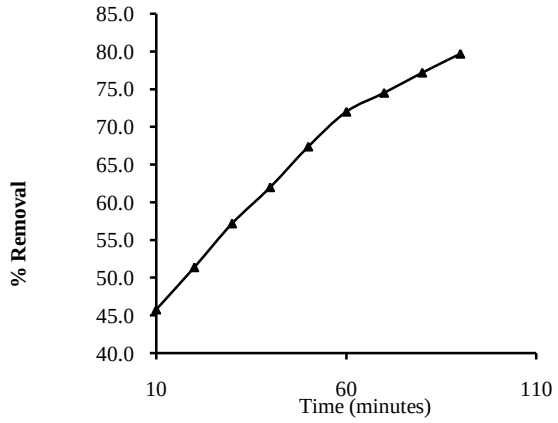

Figure 7: Effect of contact time on adsorption capacity of NAF

Conclusion

In summary, we investigated the effectiveness of Ni $Al_{0.5}$ $Fe_{1.5}O_4$ ferrite nanoparticles for removing fluoride from aqueous solution. Ni $Al_{0.5}$ $Fe_{1.5}O_4$ nanoparticles were successfully synthesized using a sol-gel method. The formation of single-phase nanosized powders was confirmed by XRD analysis as well as FTIR spectroscopy. The nanoparticles were effectively used to remove F^- ions from aqueous solution, Ni $Al_{0.5}$ $Fe_{1.5}O_4$ being the most efficient. Both the Langmuir and Freundlich adsorption isotherms fitted well for the fluoride adsorption on NAF with the regression coefficient R^2 of 0.99 and 0.95, respectively.

REFERENCES

1 R. Valenzuela, "Novel applications of ferrites," Physics Research International, vol. 2012, Article ID 591839, 9 pages, 2012

2 X. Piao, G. M. Zeng, D. L. Huang et al., "Use of iron oxide nanomaterials in wastewater treatment: a review," Science of the Total Environment, vol. 424, pp. 1–10, 2012.

3 A. K. Gupta and M. Gupta, "Synthesis and surface engineering of iron oxide nanoparticles for biomedical applications," Biomaterials, vol. 26, no. 18, pp. 3995–4021, 2005

4 Y. C. Sharma, V. Srivastava, V. K. Singh, S. N. Kaul, and C. H. Weng, "Nano-adsorbents for the removal of metallic pollutants from water and wastewater," Environmental Technology, vol. 30, no. 6, pp. 583–609, 2009

5 J.-L. Li, Z. Yu, K. Sun, X.-N. Jiang, and Z.-W. Lan, "Structural and magnetic properties of ZnFe2O4 films deposited by low sputtering power," International Journal of Minerals, Metallurgy, and Materials, vol. 19, no. 10, pp. 964–968, 2012

6 E. Avvakumov, M. Senna, and N. Kosova, Soft Mechanochemical Synthesis: A Basis for New Chemical Technologies, Kluwer Academic Publishers, Boston, Mass, USA, 2001

7 V. Šepelák, M. Menzel, K. D. Becker, and F. Krumeich, "Mechanochemical reduction of magnesium ferrite," Journal of Physical Chemistry B, vol. 106, no. 26, pp. 6672–6678, 2002.

8 Yadav, A.K, Khan, P., 2010. Fluoride and Fluorosis Status in Groundwater of Todaraisingh Area of District Tonk (Rajasthan, India): A Case Study. Int. J. Chem. Environ. Pharma. Res.; 1(1): 6-11

9 Wang, S.G., Li, Y.H., Zhao, D., Xu, C.L., Luan, Z.K., Liang, J. and Wu, D.H. (2002) Preparation of Alumina Supported on Carbon Nanotubes and Its Application in Fluoride Adsorption from an Aqueous Solution. Chinese Science Bulletin, 47, 722-724

10 Ö. Gerçel and H. F. Gerçel, "Adsorption of lead(II) ions from aqueous solutions by activated carbon prepared from biomass plant material of *Euphorbia rigida*," Chemical Engineering Journal, vol. 132, no. 1–3, pp. 289–297, 2007

11 K. Maaz, S. Karim, A. Mashiatullah, J. Liu, M.D. Hou, Y.M. Sun, J.L. Duan, H.J. Yao, D. Mo, Y.F. Chen 2009 Physica B: Condensed Matter 404 3947–3951.

12 B.D. Cullity, Elements of X-ray Diffraction, 2nd ed. Addison-Wesley, Reading, MA, 1978

13 Manish Srivastava, S. Chaubey, Animesh K. Ojha, 2009 Materials Chemistry and Physics118 174–180

14 G. Alagumuthu, V. Veeraputhiran, and R. Venkataraman, "Fluoride sorption using cynodon dactylon—based activated carbon," Hemijska Industrija, vol. 65, no. 1, pp. 23–35, 2011.